A Constant-Momentum/Energy-Selector Time-of-Flight Mass Spectrometer

C. P. Santacruz
Departamento de Fisica, Escuela Politécnica Nacional, Quito, Ecuador

P. Håkansson
Division of Ion Physics, Ångström Laboratory, Uppsala, Sweden

D. F. Barofsky
Department of Chemistry, Oregon State University, Corvallis, Oregon

C. K. G. Piyadasa
Department of Physics, University of Colombo, Colombo, Sri Lanka

A matrix assisted laser desorption/ionization time-of-flight mass spectrometer has been built with an ion source that can be operated in either constant-energy or constant-momentum acceleration modes. A decreasing electric field distribution in the ion-accelerating region makes it possible to direct ions onto a space-focal plane in either modes of operation. Ions produced in the constant-momentum mode have velocities and, thus, flight times that are linearly dependent on mass and kinetic energies that are inversely dependent on mass. The linear mass dispersion doubles mass resolving power of ions accelerated with space-focusing conditions in constant-momentum mode. The mass-dependent kinetic energy is exploited to disperse ions according to mass in a simple kinetic energy filter constructed from two closely spaced, oblique ion reflectors. Focusing velocity of ions of the same mass can substantially improve ion selection for subsequent post source decay or tandem time-of-flight analyses. (J Am Soc Mass Spectrom 2007, 18, 92–101) © 2007 American Society for Mass Spectrometry

Mass spectrometry (MS) includes a broad range of instruments and methodologies used to elucidate the structural properties of molecules, to identify the compounds present in physical and biological matter, and to quantify the chemical substances found in samples of such matter [1]. Mass spectrometers based on time-of-flight (TOF) analysis are currently playing a major role in the revolutionary expansion of mass spectrometric applications into molecular-biological research and biotechnology [2].

Essentially all TOF mass spectrometers used today in analytical applications function in what is referred to as constant-energy mode [3]. In this mode, a spatially restricted ensemble of ions in vacuum is subjected to a constant force over some fixed distance. This condition assures that essentially the same amount of work is performed, irrespective of individual mass, on all ions in the ensemble and, therefore, that they acquire, on average, the same kinetic energy. The m/z values of the ions can be determined, therefore, simply by measuring

their successive transit times over some fixed drift-distance through a flight tube to a detector. Variations around the average flight time of a set of ions having a given m/z value reflect mainly the ions' distributions in space and velocity before acceleration. When ions originate from an electrode in an accelerating region as a result, for example, of having irradiated a sample with a short burst of photons or energetic particles, their initial time and spatial distributions along the direction of acceleration are narrow, but their initial distribution in velocity is broad and somewhat mass-dependent [4]. When ions are produced in an external ion source, for example by electrospray ionization (ESI) or atmospheric pressure matrix-assisted laser desorption/ionization (MALDI), and transported orthogonally into the acceleration region [5], their initial time and velocity distributions along the direction of acceleration are narrow, but their initial spatial distribution is broad. Correction for either the wide velocity distribution in the former case or the wide spatial distribution in the latter case can be achieved to some degree by using two stages of acceleration [3]. The distance between the acceleration electrodes, the magnitudes of the accelerating potentials, and the timing and duration of voltage switching depend on whether the dual-stage accelerator is being

used to correct for an initial velocity or spatial distribution. Comprehensive descriptions of the principle of dual-stage acceleration have been written [6, 7].

It is also possible for a TOF mass spectrometer to be operated in a constant-momentum mode. Constant-momentum TOF MS was first demonstrated in 1953 by Wolff and Stephens [8]. Since that time, the potential use of constant-momentum acceleration has been discussed in the literature on a few occasions from theoretical perspectives [9–11]. In constant-momentum mode, a bunch of ions is accelerated for some fixed time. If the extraction pulse is on when the last of the ions pass through the exit grid into the field free region, they will have acquired constant energies. However, if the extraction pulse is turned off before any of the ions reach the exit grid, the same impulse is performed on all ions, irrespective of individual mass and, therefore, they will have acquired the same momenta. The linear mass-dependent velocity can be used to determine the m/z values of the ions by measuring their flight times over some fixed drift distance. The linear mass dispersion doubles the mass resolving power of ions accelerated with space-focusing conditions in constant-momentum mode. Besides, the mass-dependent kinetic energy can be exploited to disperse ions according to mass in a simple kinetic energy filter.

Currently, as far as the present authors know, there are no commercially available TOF mass spectrometers based on constant-momentum acceleration. This might be due in part to the fact that correction for an initial distribution of velocities or starting positions using constant-momentum acceleration in a uniform electric field is impossible because the kinetic energies of all ions of the same mass are increased in this acceleration mode by exactly the same amount regardless of their initial starting positions. Use of a two-stage ion reflector has been proposed as a means for correcting an initial velocity distribution in a homogeneous single-field ion source operated in a constant-momentum acceleration mode [10], but no practical device seems to have been built yet.

An alternative to using acceleration in uniform electric fields to correct for an initial distribution in velocity or space is to use acceleration in nonlinear electric fields. Methods for using nonlinear ion acceleration to improve mass resolution have been described in conjunction with both constant-energy [12] and constant-momentum mode [10, 11]. Ionaoviciu demonstrated theoretically that a modified quadrupole trap could serve to correct for an initial velocity distribution in a set of ions accelerated to constant-momentum; however, Ioanoviciu did not discuss correction for an initial spatial distribution. By virtue of its geometry, Ioanoviciu's quadrupolar arrangement of electrodes would not permit operation in both constant-energy and constant-momentum modes.

Performing multiple stages of analysis in tandem can significantly enhance the utility of mass spectrometry. Recently, two forms of tandem TOF mass spectrometers have emerged independently to set new standards for qualitative mass spectrometry. The first of these is a hybrid configuration that combines the power of quadrupole and TOF analyzers (Q-TOF) [13, 14]. The Q-TOF geometry, which can be used with ESI, MALDI, and other ionization processes, selects precursor ions with a high-performance quadrupole mass filter, fragments them via low-energy collision induced dissociation (CID), and analyzes the product-ions with a reflectron-TOF mass analyzer. The second form of tandem TOF mass spectrometry to appear in the last few years is the dual TOF [15–17]. The dual TOF geometry, which can be used with MALDI in conjunction with axial ion extraction or with ESI, MALDI, and other ionization processes in conjunction with orthogonal ion extraction [18], selects precursor ions by taking advantage of the inverse dependence of their velocities in the constant-energy mode on the square root of their masses, fragments them via high-energy CID, and after subjecting them to a second stage of acceleration, analyzes the product ions with a reflectron-TOF mass analyzer. Accelerating the product ions to energies of the order of 20 keV before analyzing them in the second mass spectrometer stage (MS_2) makes it possible to achieve high-resolution mass spectra that cover the entire mass range of the product ions and their precursor ion without stepping the voltage of the ion reflector, which is an exceptionally inefficient, tedious, manual form of scanning. Using a novel design and operational principle, it is possible to build the velocity selector used in the first stage (MS_1) so that it can choose precursors at resolving powers approaching 5000 [19]; in practice, however, velocity selectors in commercially available instruments are typically operated at resolving powers less than 500 [20].

In the present study, a simple prototype MALDI TOF mass spectrometer was constructed with an ion source that can be operated in either a constant-energy or a constant-momentum acceleration mode. The ion source is constructed so that as the electric field distribution in the ion-accelerating region is decreasing; this geometry makes it possible to direct ions onto a space-focal plane in either acceleration mode. The instrument also features an energy-selective device that, when used in combination with constant-momentum acceleration, can function as a MS_1 stage in a tandem TOF mass spectrometer. The instrument's construction, operating principles, and performance in a series of initial tests are described, and its possible uses in conjunction with axial and orthogonal ion extraction in various TOF and tandem TOF configurations are outlined.

Experimental

Sample Preparation

Solutions of 20 g/L of α-cyano-4-hydroxycinnamic acid (CHCA, Fluka Chemie GmbH, Buchs, Switzerland) in 50% methanol were used as the MALDI matrices. PEG
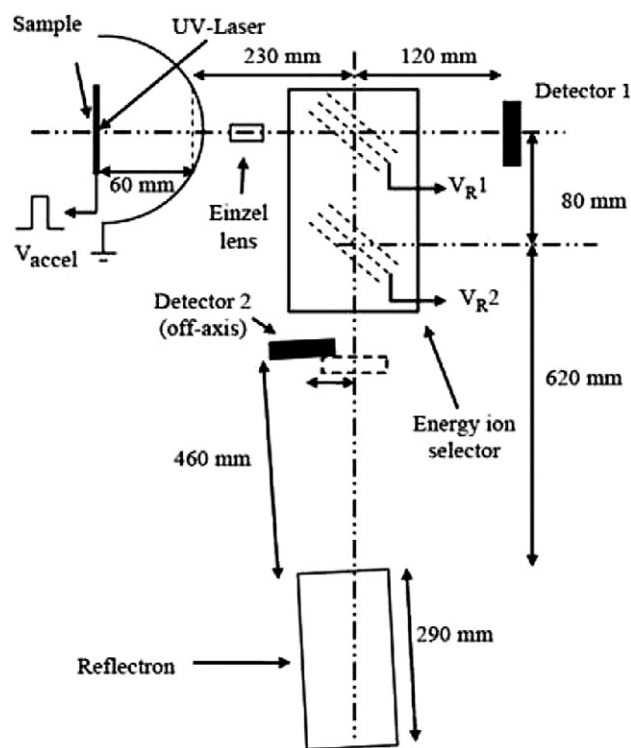
Figure 1.   Prototype MALDI TOF mass spectrometer featuring an ion source with a decreasing accelerating field, an energy-filter for selecting precursor ions, and a single-stage electrostatic mirror.

1000 (Sigma Chemical Co., St. Louis, MO) was dissolved in 30% methanol to a concentration of 10^{-4} M. Angiotensin I, substance P, neurotensin, and LHRH (Sigma) were dissolved in water/0.1% TFA to a concentration of about 10^{-5} M. NaCl and LiCl were added to some samples in amounts sufficient to generate $[M + Na]^+$ and $[M + Li]^+$ signals of approximately the same strength as the $[M + H]^+$ signal. Samples were introduced into the mass spectrometer by mixing 10 μL of matrix solution with 5 μL of analyte, depositing 3 μL of this mixture onto a metallic holder, and allowing it to dry at room temperature.

The Spectrometer

All experiments were carried out on the prototype MALDI time-of-flight mass spectrometer diagrammed in Figure 1. The MALDI ion source was constructed by locating the metallic sample support (75 × 75 mm) on the axis of a cylindrical vacuum chamber with a diameter of 150 mm and placing a flat grid with a transmission of 90% across the port leading from the ionization chamber into the flight tube. The separation between the sample support and the exit grid was 60 mm. Ion accelerating voltage pulses were generated by connecting the sample plate to a 30 kV power supply (Wallis HiVolt, Worthing, England) through a high-voltage switch (HTS-301-03GSM, Behlke Electronic GmbH, Kronberg, Germany). Accelerating potentials ranging

from 5 to 10 kV were used in all experiments. A pulse generator (DG535, Stanford Research Systems, Sunnyvale, CA) was used to control the timing of the high-voltage switch. A 337-nm, nitrogen laser with pulse width <4 ns and average power >7.2 mW/pulse (VSL-337-ND-S, Laser Science Inc., Franklin, MA) was used to ionize the samples.

After the ion source and before the ion-selector device, an Einzel lens that reduces the ions' radial velocity was located. The ion source was separated from the flight tube by an energy selector (Figure 1) consisting of a pair of 90° ion reflectors aligned in tandem at 45° to the axis of the ion beam exiting the ion source. Each reflector was constructed from three, 90% transmission, flat grids spaced 4 mm apart. A 5 kV power supply (5 kV Dual power supply, Ortec, Oak Ridge, TN) was connected to the middle grid of each reflector.

The TOF-analyzer incorporated a 290 mm long single-stage electrostatic ion reflector and two dual micro-channel plate detectors. The first detector was mounted on axis with the ion source 0.35 m from the exit grid (Detector 1). The second detector was mounted so that could be moved between a position on the axis of the reflectron to one slightly off the reflectron axis (Detector 2). With Detector 2 in the on-axis position, the instrument was operated as a short (0.35 m), straight TOF analyzer, and with the Detector 2 in the off-axis position, the instrument was operated as a much longer, reflectron TOF analyzer (Figure 1). Ion signals were acquired with an oscilloscope (500 MHz, Tektronic 520, Tektronix Inc., Wilsonville, OR) with 2 ns resolution and subsequently transferred to a computer for display analysis.

Ion Optics

The discussion in the following subsections does not take into account initial ion distributions in space and velocity; consequently, the equations presented only describe first-order effects in ion behavior.

Constant-Energy Mode

As previously stated, all TOF mass spectrometers being commercially built today operate in a constant-energy mode. When an ion with mass m, charge q, and zero initial velocity is accelerated in a uniform, static electric field E over a fixed distance d, the kinetic energy T it acquires is given by

$$T = \frac{1}{2}mv^2 = qEd \qquad (1)$$

Since the work qEd performed on the ion is independent of its mass, the kinetic energy gained in the field E by any other ion accelerated from the same starting position over the same distance d, irrespective of its mass, would also be qEd (ergo, the terminology "constant-

energy acceleration mode"). It readily follows from the preceding equation that the ion's speed v is

$$v = \left(\frac{2qEd}{m}\right)^{1/2} \tag{2}$$

and its time-of-flight t over a field-free path length L is

$$t = \frac{L}{v} = \frac{L}{(2qEd)^{1/2}} m^{1/2} \propto m^{1/2} \tag{3}$$

Hence, as is well known, a TOF mass spectrometer operating in constant-energy mode generates a mass spectrum whose mass scale is, to the first-order, proportional to the square of the flight-time, i.e., t^2, and whose mass-resolving power is half its time-resolving power, i.e., $R_{CE} = m/\Delta m = 1/2\, t/\Delta t$. Generally, mass calibration in the constant-energy mode can be based on a polynomial in $(m/z)^{1/2}$ of the form

$$t = a\left(\frac{m}{z}\right)^{1/2} + b, \tag{4}$$

where a and b are empirical constants that depend on the geometry, voltage, and timing of the instrument and that can be determined by running calibration samples [21].

Constant-Momentum Mode

When an ion with mass m, charge q, and zero initial velocity is accelerated in a uniform, static electric field E for a fixed time τ, the momentum p it acquires is given by

$$p = mv = qE\tau \tag{5}$$

The pulse duration τ must be shorter than the time it takes for the ion to exit the acceleration region. Since the impulse $qE\tau$ received by the ion is independent of its mass, the momentum gained in the field E by any other ion accelerated over the time τ, irrespective of its mass or starting position, would also be $qE\tau$ (ergo, the terminology "constant-momentum acceleration mode"). It readily follows from the preceding equation that the ion speed v is

$$v = \frac{qE\tau}{m}, \tag{6}$$

and its time-of-flight t over a path length L is

$$t = \frac{L}{v} = \frac{L}{qE\tau} m \propto m. \tag{7}$$

Hence, a TOF mass spectrometer operating in this constant-momentum mode generates a mass spectrum

whose mass scale is to the first-order linearly proportional to the flight-time t and whose mass resolving power equals its time resolving power, i.e., $R_{CM} = m/\Delta m = t/\Delta t$. Therefore, on a TOF instrument capable of operating in both constant-momentum and constant-energy accelerating modes, the mass resolving power in the former mode should be twice that in the latter mode, i.e., $R_{CM} = 2\,R_{CE}$, if the time spread is the same in both cases.

Based on eq 7, a linear polynomial in m/z of the form

$$t = c\frac{m}{z} + d \tag{8}$$

should provide suitable mass-calibration in the constant-momentum mode.

Space Focusing

In an ideal TOF analysis, the ensemble of ions would originate at the same time with zero initial velocities in a single plane in space and, subsequently, would acquire velocities that depend strictly on their respective masses. In any real MALDI TOF analysis, the ions are created at different times with nonzero initial velocities in a small volume of space. As a result, during acceleration, the ions acquire velocities that have second and higher order dependencies on mass and other factors [22]. The mass resolution, mass accuracy, and sensitivity of the subsequent mass analysis are determined in large part by the degree to which the mass spectrometer's ion optics correct for the deviations from the ideal conditions for TOF analysis. In constant-energy mode, it has become conventional to accelerate the ions in two successive, uniform electric fields to achieve space focusing on some plane along the flight axis beyond the ion source that corrects to some degree for either an initial velocity distribution or an initial spatial distribution—corrections for both initial conditions cannot be achieved simultaneously [6, 7].

In the constant-momentum mode, it is impossible to correct for an initial distribution of velocities or starting positions by accelerating the ions in a uniform electric field because all ions of the same mass gain exactly the same kinetic energy (viz. $p^2/2m = (qE\tau)^2/2m$) regardless of their initial conditions. Corrections for one or the other of these initial conditions can be achieved, however, when the ions are subjected to acceleration in a decreasing electric field. To derive mathematical formulas is beyond the scope of this article, however the fundamental idea of space focusing is given next. Ions with a given mass-to-charge ratio having initial positions within a region with a higher electric field acquire higher kinetic energies when they are accelerated for a given time (constant-momentum) or for a given distance (constant-energy) in a decreasing electric field. Thus, ions initially closer to the high voltage electrode acquire higher kinetic energies than ions originally closer to the grounded grid. The initial kinetic energy

distribution of ions could be converted to space distribution using a delayed extraction technique. Thus, some space focusing is achievable using the dependence of the final ion velocity on the initial position in either constant-energy or constant-momentum mode. In the constant-energy mode, the position of the space-focal plane, for ions that originate either with an initial velocity distribution from the plane of the sample plate or with an initial spatial distribution from a continuous beam entering the accelerator orthogonal to the time-of-flight axis, can be set by varying the delay of the voltage pulse used to produce the decreasing accelerating field. Alternatively, the same end can be achieved in the constant-momentum mode by varying both the delay and duration of the voltage pulse. Optimum focusing conditions depend on the characteristics of the electric field and operating conditions, and they may be found through a rigorous mathematical treatment that will be discussed in following articles.

The ion-source geometry shown in Figure 1 is a particular example of a configuration that has a decreasing, nonlinear electric field. With this ion source, the mode of acceleration can be changed from constant-energy to constant-momentum or vice versa at any time before or during operation simply by changing the duration of the voltage pulse applied to the sample plate. Space focusing can be achieved in either constant-energy or constant-momentum modes. The only requirement imposed on any ionization process used with a system like the one shown in Figure 1 is that the ions should be generated in the plane of the sample plate (as would be the case, for example, with MALDI or any particle-induced desorption/ionization process), or that the ions should be introduced into the extraction region along an axis that lies close to the plane of the sample plate (as would be the case, for example, with ESI, high-pressure MALDI, or any other continuous or quasicontinuous ionization process).

Results and Discussion

Mass Resolving Power

A set of experiments using LHRH (1182.3 Da) and angiotensin I (1296.5 Da) were performed with the prototypical system (Figure 1) to observe the relative effects of acceleration voltage, voltage pulse delay time, and voltage pulse duration on mass resolving power. Space-focused spectra were recorded in both accelerating modes at Detector 1. This was accomplished in the constant-energy mode by measuring the mass resolving power as a function of voltage pulse delay and in the constant-momentum mode by measuring the mass resolving power as a function of both voltage pulse delay and voltage pulse duration.

On any particular TOF analyzer with a given time resolving power $t/\Delta t$, the mass resolving power R_{CM} in a constant-momentum accelerating mode should, theoretically, as demonstrated in a preceding section, be
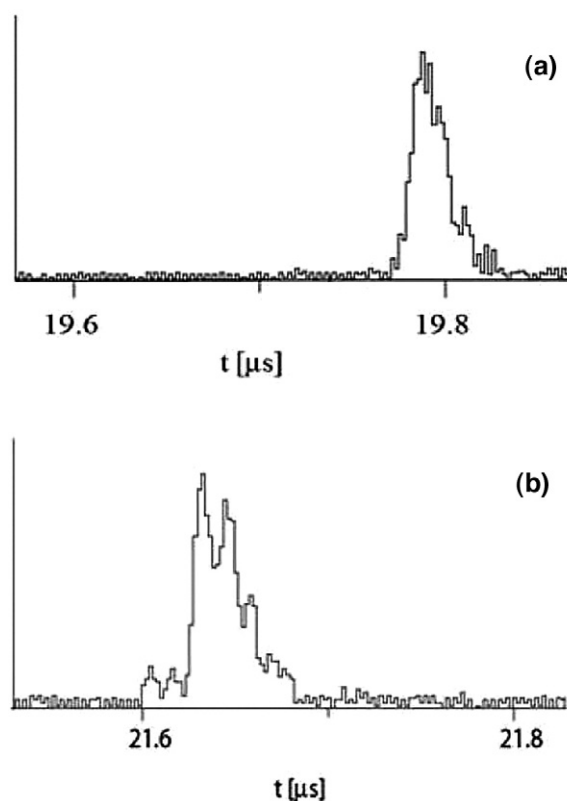

Figure 2. MALDI spectra of LHRH (1182.3 Da) recorded under space-focusing conditions at Detector 1 located at 0.35 m from the exit grid: (**a**) constant-energy accelerating mode with V_{accel} = 9 kV and τ_{delay} = 580 ns and (**b**) constant-momentum accelerating mode with V_{accel} = 9 kV, τ_{delay} = 1370 ns, and τ_{accel} = 2200 ns.

double the mass resolving power R_{CE} in a constant-energy accelerating mode. MALDI spectra recorded in both the constant-energy and constant-momentum modes were calibrated using the LHRH and its sodium adduct to find the coefficients of eq 4 and eq 8, respectively. Then, the mass resolving power of the molecular ions of LHRH was calculated. The FWHM mass resolving power estimated from the LHRH peak recorded in the constant-energy mode (Figure 2a) is R_{CE} = 680, whereas the FWHM resolving power computed from the corresponding peak recorded in the constant-momentum mode (Figure 2b) is R_{CM} = 1100. Several spectra at different acceleration voltages show similar results. The average ratio R_{CM}/R_{CE} of these two values is 1.6 ± 0.1; within the margin of experimental error, this value is close, but lower, to the theoretically predicted value of 2.

To eliminate the possibility that the factor of 1.6 could be caused by an inherently more advantageous configuration of the source for the constant-momentum mode, the system was studied by simulation (SIMION 7) considering ions with different initial kinetic energies (range between 0 to 10 eV) and different initial positions (range between 0 to 1 mm). According to the simulations, under space focusing conditions, the time spread of an ion bunch is similar in both constant-momentum
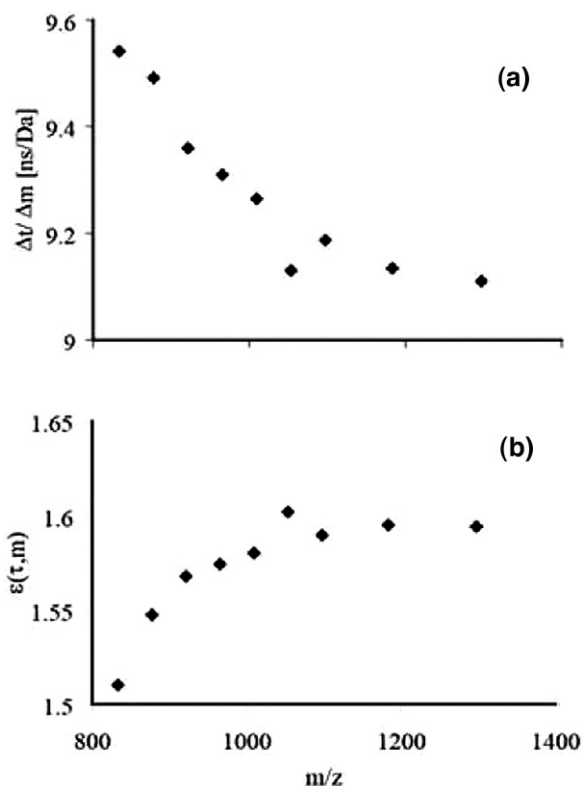
Figure 3. Plot of the ratio $\Delta t/\Delta m$ versus m/z for PEG 1000 ions recorded in the constant-momentum mode with $V_{accel} = 5$ kV, $\tau_{delay} = 1600$ ns, and $\tau_{accel} = 2700$ ns (**a**). Plot an estimation of the parameter that considers the effects of the variation of the electric field (**b**).

and constant-energy modes. Thus, we believe that the factor of 1.6 reflects an increase caused by the constant-momentum mode. However, the experimental focusing characteristics of the source could not be the most favorable for the constant-energy mode.

Mass Calibration

In principle, flight-time in the constant-momentum accelerating mode is a linear function of mass as expressed by eq 7 or eq 8; however, the initial velocity distribution the ions receive during the MALDI event, the decreasing electric field and, probably, other factors give rise to a deviation in this linear relationship.

The dependence of flight-time on mass in constant-momentum mode was studied by measuring the flight-times of PEG 1000, angiotensin I, LHRH, and substance P to Detector 1. The space focusing conditions to run the experiments were optimized for ions around 1000 Da. The ratio $\Delta t/\Delta m$ for the evenly spaced PEG 1000 ions (44 u apart) was found to decrease with the mass (Figure 3a). This deviation from linearity can be explained by the combined effects of the ions' initial velocity distribution and the variation of the electric field.

The component of momentum along the axis of the

ion source received by any ion, regardless of the actual shape of $E(x)$, can always be expressed as

$$p_{accel} = \varepsilon(\tau, m) = \frac{qV\tau_{accel}}{d} = \varepsilon(\tau, m)p_{uniform} \qquad (9)$$

where $\varepsilon(\tau, m)$ takes into account the effects of the decreasing electric field, and τ_{accel} is the voltage-pulse duration. From this expression and considering the initial velocity v_0 of MALDI ions, it follows that the velocity of the ions after acceleration is

$$v = v_0 + \frac{p_{accel}}{m} = \frac{\varepsilon(\tau, m)p_{uniform}}{m}\left(1 + \frac{mv_0}{\varepsilon(\tau, m)p_{uniform}}\right). \qquad (10)$$

The total time an ion spends in flight following the laser pulse is therefore given by

$$t_{total} = \tau_{delay} + \tau_{accel} + \frac{L + d - x_{accel}(\tau, m)}{\dfrac{\varepsilon(\tau, m)p_{uniform}}{m}\left(1 + \dfrac{mv_0}{\varepsilon(\tau, m)p_{uniform}}\right)} \qquad (11)$$

where τ_{delay} is the voltage-pulse delay, and $x_{accel}(\tau, m)$ is the position after acceleration. Considering that $mv_0/\varepsilon(\tau, m)p_{uniform} \ll 1$, the last equation can be expanded in a Taylor's series to give

$$
\begin{aligned}
t_{total} = {}& \tau_{delay} + \tau_{accel} + \frac{L + d - x(\tau, m)}{\varepsilon(\tau, m)p_{uniform}} \\
& \times \left[m - \left(\frac{v_0}{\varepsilon(\tau, m)p_{uniform}}\right)m^2 \right. \\
& + \left(\frac{v_0}{\varepsilon(\tau, m)p_{uniform}}\right)^2 m^3 \\
& \left. - \left(\frac{v_0}{\varepsilon(\tau, m)p_{uniform}}\right)^3 m^4 + \cdots \right]
\end{aligned}
\qquad (12)
$$

Considering that the variation of $L + d - x(\tau, m)$ and $\varepsilon(\tau, m)$ are slowly varying functions of mass, the differential of t_{total} yields

$$
\begin{aligned}
\frac{\Delta t_{total}}{\Delta m} = {}& \frac{L + d - x(\tau, m)}{\varepsilon(\tau, m)p_{uniform}}\left[1 - 2\left(\frac{v_0}{\varepsilon(\tau, m)p_{uniform}}\right)\right. \\
& \left. \times m + 3\left(\frac{v_0}{\varepsilon(\tau, m)p_{uniform}}\right)^2 m^2 \right]
\end{aligned}
\qquad (13)
$$

Adjusting the experimental results of Figure 3a by using the last equation and considering the initial velocity v_0 around 1000 m/s, it turns out that the parameter $\varepsilon(\tau, m)$ falls within the range $1.5 < \varepsilon(\tau, m) < 1.6$ but becomes nearly constant at $\sim m/z$ 1100 (Figure 3b). Thus,

Table 1. Calibrated spectrum of PEG 1000, LHRH, angiotensin I and substance P ions using a linear relation between mass and flight-time

Theoretical mass	Constant-momentum			
(Da)	Linear calibration	Error (Da)	Quadratic correction[a]	Error (Da)
833.95	832.53	−1.42	833.44	-0.51
878.00	878.00	—	878.00	—
922.06	923.26	1.20	922.51	0.45
966.11	967.86	1.75	966.53	0.42
1010.16	1012.25	2.09	1010.49	0.33
1054.21	1056.43	2.22	1054.39	0.18
1098.27	1099.95	1.68	1097.79	-0.48
1183.30	1185.27	1.97	1183.30	—
1297.48	1298.19	0.71	1297.35	-0.13
1349.62	1349.62	—	1349.62	—

[a]Quadratic correction reduces the rms mass error from 1.7 to 0.4 Da in a drift length of 0.35 m. V_{accel} = 5 kV, τ_{delay} = 1600 ns, and τ_{accel} = 2700 ns.

the variation of the ratio $\Delta t/\Delta m$ for the evenly spaced PEG 1000 ions (44 u apart) is caused by the dependence of t_{total} on the initial velocity and the variation of the parameter $\varepsilon(\tau, m)$ with the mass. Therefore, the relationship between mass and flight-time deviates from linear. However, a linear calibration and a quadratic correction is enough to reduce the mass error. For example, fitting the mass and time data using the linear eq 8 for ions in constant-momentum mode produces a line that underestimates the mass error close to the extremes or overestimates it in the middle, figure not shown. Quadratic correction to the linear calibration using three points [23] reduces the root mean square error from 1.7 to 0.4 Da; results are shown in Table 1.

Ion Selection by Energy Filtering

In accordance with eq 5, an ion that undergoes acceleration in the constant-momentum mode emerges from the acceleration region with kinetic energy T that, to the first-order, equals $(qE\tau)^2/2m$. Since this energy is inversely proportional to mass, energy filtering can be used in combination with constant-momentum acceleration as a basis for ion selection in which the selection resolving power is $R_{Sel.} = T/\Delta T$. To test this capability, a simple energy filter was constructed from two tandem ion reflectors. In this configuration, the first reflector acts as a high-energy cut-off filter in which all ions with energies greater than $2qV_{R1}$, where q is the charge and V_{R1} is the voltage applied to the first reflector's retarding grid, pass through the analyzer. All ions with energies less than $2qV_{R1}$ are reflected through 90° toward the second ion reflector. The second reflector acts as a low-energy cut-off filter in which all ions with energies less than $2qV_{R2}$, where V_{R2} is the voltage applied to the second reflector's retarding grid, are reflected through 90° off the flight path of the TOF

section. All ions with energies greater than $2qV_{R2}$ pass through the analyzer and continue towards the detector. The two reflectors operating in tandem form an ion selector with an energy window equal to $2q(V_{R1}–V_{R2})$; by adjusting the two retarding potentials V_{R1} and V_{R2}, this window can easily be made arbitrarily wide or narrow as well as centered on any energy in the range of the extracted ions. When the MALDI ion source is operated in the constant-energy mode under space-focusing conditions, and the energy-selector's window is centered on $1/2qV_{accel}$, where V_{accel} is the magnitude of the voltage pulse used to accelerate the ions out of the source, the system functions as a conventional constant-energy MALDI TOF mass spectrometer. By narrowing the selector's window under the preceding conditions and using the 180° reflectron (Detector 2 in off-axis position), mass resolving power can be increased substantially, albeit at the expense of ion transmission, i.e., sensitivity.

Use of the energy filter as a simple ion selector in conjunction with constant-momentum acceleration is illustrated by the mass spectra of PEG 1000 exhibited in Figure 4a. In this example, all of the PEG ions in the sample, regardless of mass, could be transmitted to Detector 2 in its on-axis position and recorded by applying more than 3000 V (roughly half the potential used to accelerate the ions) to the first reflector (V_{R1}) and grounding the second reflector (V_{R2} = 0 V). From this state, the filter could readily be transformed into a high-mass ion selector (i.e., low-energy ions) by decreasing V_{R1} slightly while leaving V_{R2} at ground potential (Figure 4b) or a low-mass ion selector (i.e., high-energy ions) by increasing V_{R2} a bit while leaving V_{R1} at its original setting (Figure 4c). Finally, the filter could be turned into a limited-mass-range ion selector by both decreasing V_{R1} increasing V_{R2} somewhat from their original values (Figure 4d).

Space focusing requires that a velocity distribution Δv be generated during either constant-energy or constant-momentum acceleration; hence, acceleration intended to achieve space focusing would be more aptly termed pseudoconstant energy or pseudo constant-momentum, respectively. In the case of constant-momentum acceleration, this space focusing Δv translates into a kinetic energy distribution ΔT, which for the purposes of ion selection based on energy filtering, inescapably places an upper limit on the selection resolving power. If, instead of setting the ion source's operating parameters to achieve space focusing for a particular mass, those parameters are adjusted to minimize Δv for that same mass, i.e., achieve focusing velocity, ΔT can be reduced and, thereby, the selection resolving power increased to a considerable degree.

In the ion source (Figure 1), switching from space focusing to focusing velocity in the constant-momentum accelerating mode requires changing both the delay and duration of the accelerating pulse. By setting the mass window of the energy selector on the molecular ion envelope and adjusting the delay time for
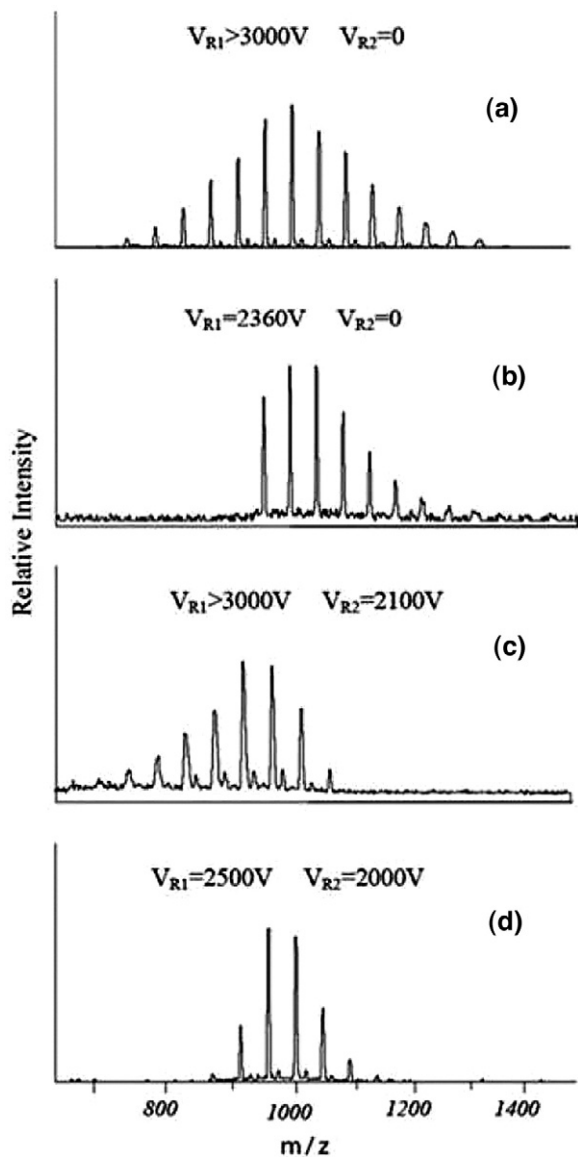
Figure 4. Energy ion selection of PEG 1000 ions in constant-momentum mode: V_{accel} = 6 kV, τ_{delay} = 1500 ns, and τ_{accel} = 2300 ns. No ion selection: V_{R1}>3 kV and V_{R2} = 0 (**a**). Removal of high-energy ions: V_{R1} = 2360 V and V_{R2} = 0 (**b**). Removal of low-energy ions: V_{R1}>3 kV and V_{R2} = 2100 V (**c**). Selection of a mass range: V_{R1} = 2500 V and V_{R2} = 2000 V (**d**).

maximum resolving power, focusing velocity was readily achieved for the different analytes with the instrument configured as a short, straight TOF analyzer, i.e., with the Detector 2 (Figure 1) in the on-axis position (0.35 m flight path). Isolation of the different cationized forms produced from a sample of LHRH containing small amounts of NaCl and LiCl provides an example of the ion selector's basic operation (Figure 5). With the first ion mirror set at a potential that reflects all ions regardless of mass, and the second ion mirror grounded, the instrument recorded a full spectrum (Figure 5a). Decreasing the first mirror's potential by a few hundred volts eliminated [LHRH + H]$^+$ from the spectrum (Figure 5b) reducing the first mirror's poten-

tial by another 20 V and setting the second mirror's potential for an energy window of 80 eV selected [LHRH + Na]$^+$ (Figure 5c). Finally, narrowing the ion selector's energy window to 50 eV and shifting it upward by 200 eV centered it on [LHRH + H]$^+$ without reducing ion transmission appreciably (Figure 5d).

Whereas the preceding example with LHRH demonstrated how the energy filter selects focused ions in the constant-momentum mode, it did not show the system's potential for high selection resolving powers because the effect of focusing velocity was entirely
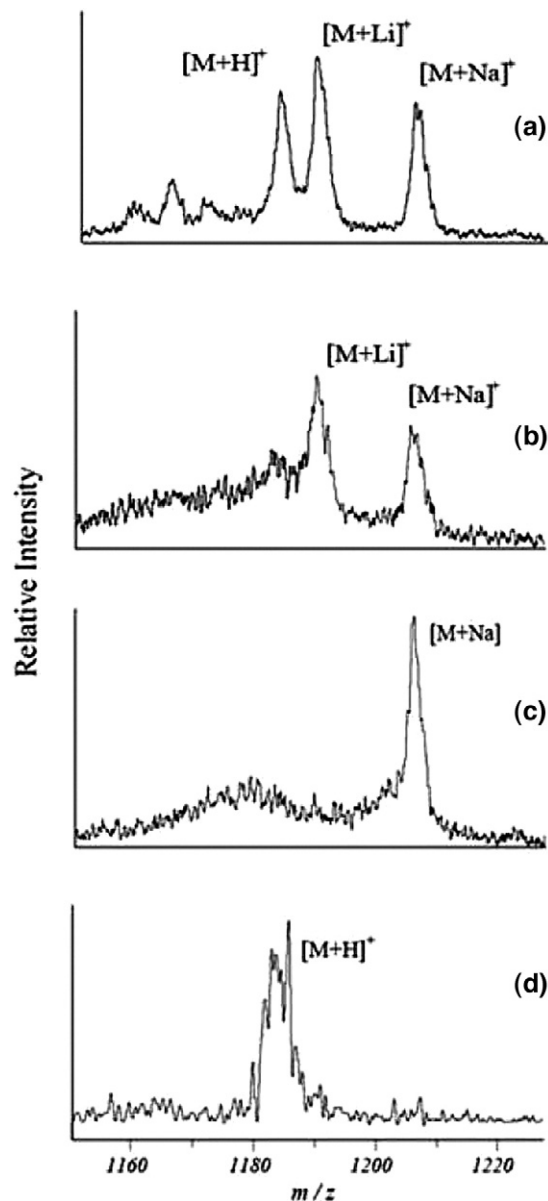

Figure 5. Constant-momentum mass spectra of a sample of LHRH (1182.3 Da) containing small amounts of LiCl and NaCl and using focusing velocity. Full spectrum: V_{accel} = 9.9 kV, τ_{delay} = 2200 ns, τ_{accel} = 1000 ns, Einzel lens potential = 5 kV, V_{R1} > 4300 V, V_{R2} = 0 V (**a**); spectrum with [LHRH + H]$^+$ removed: V_{R1} = 4050 V, V_{R2} = 0 V (**b**); spectrum with [LHRH + Na]$^+$ selected: V_{R1} = 4030 V, V_{R2} = 3950 V (**c**); spectrum with [LHRH + H]$^+$ selected: V_{R1} = 4230 V, V_{R2} = 4180 V (**d**).

Table 2. Effect of Einzel lens on pseudo kinetic energy distribution of approximately 5000 eV measured on Detector 2 (on-axis position, 0.35m), constant-momentum LHRH ions: V_{accel} = 6 kV, τ_{delay} = 1500 ns, and τ_{accel} = 2300 ns

Einzel lens potential [V]	E [eV]
0	150
3000	50

masked by peak broadening due to the large radial velocity distribution created by MALDI. Ions with appreciable, radial velocity components traverse significantly longer paths through the ion selector's mirrors to reach the detector and, thereby, introduce a time-spread (or pseudokinetic energy-spread) that dominates all other factors that contribute to peak broadening. The rudimentary design and construction of the prototype instrument used in this study had no provision for minimizing this effect other than the Einzel lens located between the ion source and the ion selector (Figure 1), but this device was only capable of reducing peak widths (i.e., pseudoenergy distributions) to a very limited degree. Without restricting ion transmission for example, the FWHM pseudokinetic energy distribution of 5000 eV, constant-momentum PEG 1000 ions was reduced from 150 to 50 eV at Detector 2 in the on-axis position when 3000 V was applied to the Einzel lens (Table 2).

Despite the limitations imposed by the prototype instrument's unsophisticated ion optics, it was possible to demonstrate the effect of focusing velocity and ion selector's potential for high selection resolving powers by closing down the ion selector's energy-window to values less than an electron volt. By setting the energy window this narrow, transmission was decreased to less than 10% and restricted almost exclusively to coaxial ions. By using the single-stage mirror to increase the mass resolving power (Detector 2 in off-axis position), baseline resolution of neurotensin's isotopic envelope was achieved by closing the ion selector's window for the velocity-focused ions to about 6 eV (Figure 6a), and the most abundant isotopic ion was isolated by further narrowing the window to about 0.5 eV (Figure 6b).

Although striking, the result reported in the preceding paragraph should by no means be considered routine—it required severely reducing ion transmission, considerable manual dexterity, and exceptional patience. Nevertheless, it indicates that, with proper ion-optical design, constant momentum acceleration in conjunction with energy filtering might serve as the basis for a MS_1 in a hybrid tandem TOF mass spectrometer. In an axial MALDI configuration, all of the acceleration/focusing modes described in the preceding text would apply. Operating the MALDI source in the constant-momentum mode, and the energy-selector with a narrow energy window would permit isolation of precursor ions for subsequent high-energy collision-induced dissociation analysis. Using the energy selector

for MS_1 would obviate the need for the complicated timing and high voltage switching circuitry that is required by tandem TOF systems that use lower resolution velocity selectors for MS_1. The 90° energy selector is not compatible with orthogonal extraction geometries because the relatively large velocity component of the ion beam orthogonal to the direction of ion extraction could lead to a significant loss in resolving power. It should be possible, however, to use a 180° energy selector in the orthogonal extraction geometry. In a 180° configuration, the first analyzer would act as the low-energy cut-off filter, and the second analyzer would act as the high-energy cut-off filter. Using the constant-energy mode to perform orthogonal extraction in this configuration, the system would operate the same as any conventional orthogonal extraction TOF mass spectrometer, but performing orthogonal extraction in the constant-momentum mode should increase the resolving power of the system by a factor of 2. The energy selector would be used to isolate precursor ions at high resolution for subsequent tandem mass analysis in the same way as was just described for the axial MALDI configuration.

Conclusions

The system in this report has a unique capability of producing constant-momentum ions with energy mass dependence. The ions are accelerated in a single stage, pulsed, decreasing nonlinear electric field. Changing the duration of the voltage pulse, the mode of acceler-
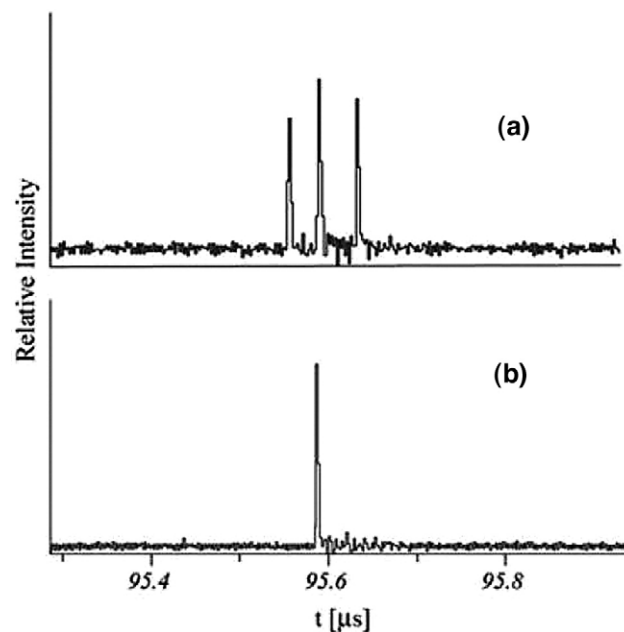

Figure 6. Constant-momentum mass spectra of neurotensin (1671.9 Da) using focusing velocity. Baseline resolved spectrum of the three most abundant isotopes of neurotensin: V_{accel} = 6 kV, τ_{delay} = 1525 ns, τ_{accel} = 2500 ns, V_{R1}–V_{R2}" 6 V (**a**); spectrum of isolated central isotope at a FWHM resolving power of 14,000: as above except V_{R1}–V_{R2}" 0.5 V (**b**).

ation can be changed from constant-energy to constant-momentum or vice versa. By varying the timing of the electric field, the ions can be spaced focused with either constant energies or constant momenta. The mass resolution of ions accelerated with space-focusing conditions in constant-momentum mode is double that in the constant energy mode. The mass scale of ions accelerated to constant-momentum is linear to the first-order, but mass calibration requires quadratic correction because of the variation of the electric field and the relatively large initial velocity distribution created by MALDI.

The mass-dependent kinetic energies of ions accelerated in constant-momentum mode can be used as the basis for ion selection. Varying the timing and duration of the decreasing electric field, the ions' velocity in constant-momentum mode can be focused. This focusing in accordance with basic ion optics reduces the kinetic energy distribution and makes it possible to achieve exceptionally high resolution ion selection with the energy filter. Even at moderate ion selector resolving powers, it should be possible to use a constant-momentum/energy-filter mass spectrometer in tandem with a TOF mass spectrometer for many applications. Different ionization systems, axial MALDI or orthogonal ESI and atmospheric pressure MALDI, could be coupled to such an instrument.

Although additional development is required to improve the shape of the electric field, the ion optics, and the efficiency of ion selection for routine analyses, a constant-momentum/energy-selector device has the potential for operational and analytical characteristics superior to any constant-energy/velocity-selecting device known to the present authors.

Acknowledgments

References

1. Matsuo, T.; Seyama, Y. Introduction to Modern Biological Mass Spectrometry. *J. Mass Spectrom.* **2000,** *35,* 114–130.
2. Costello, C. E. Bioanalytical Applications of Mass Spectrometry. *Anal. Biotechnol.* **1999,** *10,* 22–28.
3. Wiley, W. C.; McLaren, I. H. Time-of-Flight Mass Spectrometer with Improved Resolution. *Rev. Sci. Instrum.* **1955,** *26,* 1150–1157.
4. Karas, M.; Bahr, U.; Fournier, I.; Gluckmann, M.; Pfenninger, A. The Initial-Ion Velocity as a Marker for Different Desorption-Ionization Mechanisms in MALDI. *Int. J. Mass Spectrom.* **2003,** *226,* 239–248.
5. Guilhaus, M.; Selby, D.; Mlynski, V. Orthogonal Acceleration Time-of-Flight Mass Spectrometry. *Mass Spectrom. Rev.* **2000,** *19,* 65–107.
6. Cotter, R. J. Time-of-Flight Mass Spectrometry: Instrumentation and Applications to Biological Research. Am. Chem. Soc. Washington, DC, **1997,** Chap II.
7. Ioanoviciu, D. Ion-Optical Solutions in Time-of-Flight Mass Spectrometry. *Rapid Commun. Mass Spectrom.* **1995,** *9,* 985–997.
8. Wolff, M. M.; Stephens, W. E. A Pulsed Mass Spectrometer with Time Dispersion. *Rev. Sci. Instrum.* **1953,** *24,* 616–617.
9. Poschenrieder, W. P. Multiple-Focusing Time of Flight Mass Spectrometers. I. TOFMS with Equal Momentum Acceleration. *Int. J. Mass Spectrom. Ion Phys.* **1971,** *9,* 357.
10. Ioanoviciu, D. Delayed Extraction-Constant Momentum Time-of-Flight Mass Spectrometry. *Nucl. Instrum. Methods Phys. Res. A* **1999,** *427,* 157–160.
11. Ioanoviciu, D. Perfect Velocity Focusing in Hyperbolic Electrode Source-Drift Space Time-of-Flight Mass Analyzers. *Rapid Commun. Mass Spectrom.* **1999,** *12,* 1925–1927.
12. Gardnera, B. D.; Holland, J. F. Nonlinear Ion Acceleration for Improved Space Focusing in Time-of-Flight Mass Spectrometry. *J. Am. Soc. Mass Spectrom.* **1999,** *10,* 1067–1073.
13. Chernushevich, I. V.; Loboda, A. V.; Thomson, B. A. An Introduction to Quadrupole-Time-of-Flight Mass Spectrometry. *J. Mass Spectrom.* **2001,** *36,* 849–865.
14. Shevchenko, A.; Loboda, A.; Shevchenko, A.; Ens, W.; Standing, K. G. MALDI Quadrupole Time-of-Flight Mass Spectrometry: A Powerful Tool for Proteomic Research. *Anal. Chem.* **2000,** *72,* 2132–2141.
15. Vestal, M.; Juhasz, P.; Hines, W.; Martin, S. An Improved Delayed Extraction MALDI-TOF MS for PSD and CID. *Proceedings of the 46th ASMS Conference on Mass Spectrometry and Allied Topics*, Orlando, FL, 1998.
16. Katz, D.; Barofsky, D. A New Design for a MALDI Tandem Time-of-Flight Mass Spectrometer. *Proceedings of the 47th ASMS Conference on Mass Spectrometry and Allied Topics*, Dallas, TX, 1999.
17. Medzihradszky, K. F.; Campbell, J. M.; Baldwin, M. A.; Falick, A. M. Juhasz, P.; Vestal, M. L.; Burlingame, A. The Characteristics of Peptide Collision-Induced Dissociation Using a High-Performance MALDI-TOF/TOF Tandem Mass Spectrometer. *Anal. Chem.* **2000,** *72,* 552–558.
18. Barofsky,, D. F., Håkansson,, P., Katz,, D. L., Piyadasa,, C. K. G. Tandem Time-of-Flight Mass Spectrometer. U.S. Patent No. 6489610, 2002.
19. Piyadasa, C. K. G.; Håkansson, P.; Ariyaratne, T. R.; Barofsky, D. F. A high Resolving Power Ion Selector for Post-Source Decay Measurements in a Reflecting Time-of-Flight Mass Spectrometer. *Rapid Commun. Mass Spectrom.* **1998,** *12,* 1655–1664.
20. Yergey, A. L.; Coorssen, J. R.; Backlund, P. S. Jr.; Blanck, P. S.; Humphrey, G. A.; Zimmergerg, J.; Campbell, J. M.; Vestal, M. L. De Novo Sequencing of Peptides Using MALDI/TOF-TOF. *J. Am. Soc. Mass Spectrom.* **2002,** *13,* 784–791.
21. Costa-Vera, C.; Zubarev, R.; Ehring, H.; Håkansson, P.; Sunqvist B. U. R. A Three-point Calibration Procedure for Matrix Assisted Laser Desorption/Ionization Mass Spectrometry Utilizing Multiply Charged Ions and Their Mean Initial Velocities. *Rapid Commun. Mass Spectrom.* **1996,** *10,* 1429–1432.
22. Glückmann, M.; Karas, M. The Initial Ion Velocity and Its Dependence on Matrix, Analyte, and Preparation Method in Ultraviolet Matrix-Assisted Laser Desorption/Ionization. *J. Mass Spectrom.* **1999,** *34,* 467–477.
23. Hack, C.; Benner, W. H. A Simple Algorithm Improves Mass Accuracy to 50–100 ppm for Delayed Extraction Linear Matrix-Assisted Laser Desorption/Ionization Time-of-Flight Mass Spectrometry. *Rapid Commun. Mass Spectrom.* **2002,** *16,* 1304–1312.